THE COMPANY OF
Biologists

RESEARCH ARTICLE

The maternal nucleolus plays a key role in centromere satellite maintenance during the oocyte to embryo transition

Helena Fulka[1],* and Alena Langerova[2]

ABSTRACT

The oocyte (maternal) nucleolus is essential for early embryonic development and embryos originating from enucleolated oocytes arrest at the 2-cell stage. The reason for this is unclear. Surprisingly, RNA polymerase I activity in nucleolus-less mouse embryos, as manifested by pre-rRNA synthesis, and pre-rRNA processing are not affected, indicating an unusual role of the nucleolus. We report here that the maternal nucleolus is indispensable for the regulation of major and minor satellite repeats soon after fertilisation. During the first embryonic cell cycle, absence of the nucleolus causes a significant reduction in major and minor satellite DNA by 12% and 18%, respectively. The expression of satellite transcripts is also affected, being reduced by more than half. Moreover, extensive chromosome bridging of the major and minor satellite sequences was observed during the first mitosis. Finally, we show that the absence of the maternal nucleolus alters S-phase dynamics and causes abnormal deposition of the H3.3 histone chaperone DAXX in pronuclei of nucleolus-less zygotes.

KEY WORDS: Nucleolus precursor body, Centromere, Chromosome bridging, Satellite DNA, Replication stress, Mice

INTRODUCTION

The transition from meiosis to mitosis is a crucial period in animal life. Although extensively studied it is not yet completely understood. Mammalian oocytes and early embryos contain atypical nucleoli [termed nucleolus precursor bodies (NPBs)]. Unlike somatic cell nucleoli, these structures lack the three basic nucleolar compartments (fibrillar centres, granular and dense fibrillar components); instead, they are composed solely of dense fibrillar material of unknown composition (Biggiogera et al., 1994; Pochukalina and Parfenov, 2008). These atypical organelles originate from formerly transcriptionally active nucleoli of growing oocytes. Initially, oocytes increase enormously in size and synthesize large amounts of material (including rRNA), and the oocyte nucleolus structurally resembles the somatic cell-type nucleolus. When oocytes reach full size, transcription ceases and the somatic cell-type nucleolus is transformed into the NPB (Chouinard, 1971).

Interestingly, NPBs can be microsurgically removed (enucleolation) and even transplanted back into oocytes (Fulka et al., 2003; Ogushi and Saitou, 2010). Based on this experimental approach, it was shown that NPBs in zygotes are of maternal (oocyte) origin and are essential for early development: embryos originating from enucleolated oocytes are unable to replace this organelle, form nucleolus-less nuclei and are arrested at the 2-cell stage. When oocytes are enucleolated but the NPB

[1]Institute of Animal Science, CZ 104 01 Prague, Czech Republic. [2]GENNET, CZ 170 00 Prague, Czech Republic.

*Author for correspondence (hell.f@seznam.cz)

is transplanted back, healthy offspring can be obtained (Ogushi et al., 2008). The reason for the developmental arrest of nucleolus-less embryos is unclear, although it has been speculated that the problem might lie in the lack of, or aberrant, transcription. Here, we show that whereas rRNA transcription activation and pre-rRNA processing are unaffected by the absence of NPBs, this organelle is essential for the regulation of major and minor satellite sequences and consequently for normal development.

RESULTS

Early embryos use surprisingly little of the original maternal nucleolar material

Because the maternal NPB is essential for embryonic development and embryos originating from enucleolated oocytes arrest at the 2-cell stage (Ogushi et al., 2008; Ogushi and Saitou, 2010), the common view of the NPB role is that it serves as the storage site of nucleolar proteins. However, a question remains as to what extent the developing embryo is dependent on such maternal stocks or maternal mRNAs encoding nucleolar proteins. We focused on B23 [nucleophosmin 1 (Npm1)], C23 [nucleolin (Ncl)], fibrillarin (Fbl) and UBF (Ubtf), as these are by far the best-characterised nucleolar components. Interestingly, when the mRNA levels were measured we found no accumulation of these transcripts during the oocyte growth period (Fig. 1A). In fact, in the case of Ubtf and Fbl, their mRNA levels declined markedly. After fertilisation, the transcripts decreased even further, reaching the lowest levels at the 2-cell embryonic stage, when genome activation occurs in the mouse (Fig. 1B). The appearance of paternal transcripts at this stage indicates that the maternal transcripts are actually eliminated prior to this stage (Fig. 1C).

Next we asked whether the nucleolar proteins are carried over to the embryo. With the exception of B23, we found no evidence that even the proteins were accumulated by oocytes. By contrast, a clear decline in the protein levels was observed between the germinal vesicle (GV) and metaphase II (MII) oocyte stages, when fertilisation occurs (Fig. 1D). Therefore, the developing mouse embryo makes very little or no use of the maternal nucleolar proteins and their mRNAs.

Embryos successfully activate rRNA transcription and pre-rRNA processing in the absence of NPBs

To further investigate the possibility that embryos constitute fully functional nucleoli *de novo*, we examined whether rRNA production is initiated in the absence of NPBs.

To discriminate between the possible impact of the enucleolation procedure and NPB absence on rRNA synthesis, three groups of embryos were prepared. In the first group, the oocyte (maternal) NPB was removed and transplanted back, and these oocytes were allowed to mature to the MII stage and then intracytoplasmic sperm injection (ICSI) was performed. The second group was subjected to the same procedure except that the NPB was completely removed. In the third group, no manipulation was performed prior to ICSI
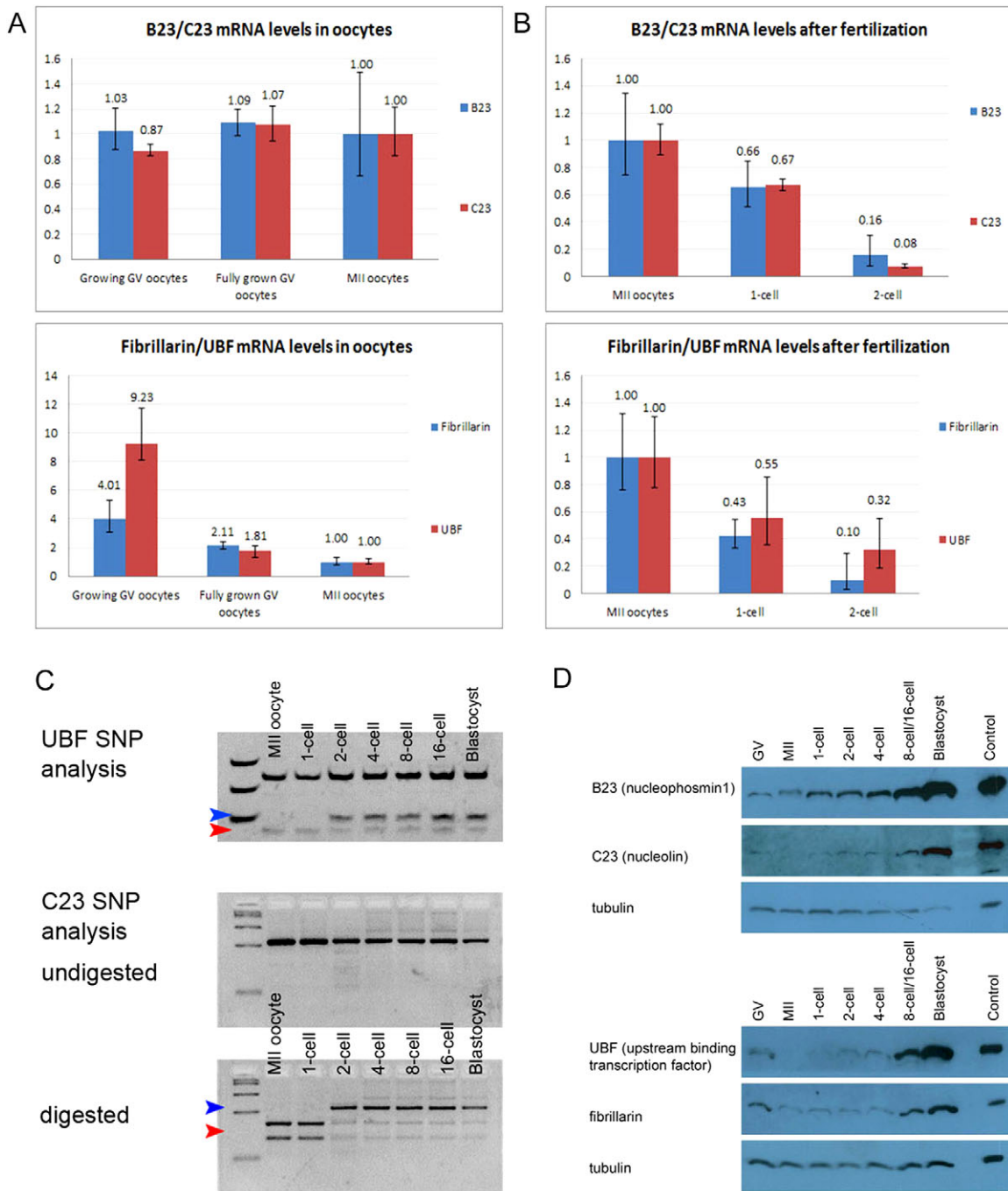
DEVELOPMENT

Fig. 1. Mouse embryos make surprisingly little use of maternal nucleolar material or nucleolar factor transcripts. (A) During final phases of growth, oocytes do not accumulate mRNAs encoding typical nucleolar proteins. In fact, as they reach MII, *Ubtf* and *Fbl* mRNAs are largely degraded (≥45 oocytes analysed in each group). (B) The mRNA levels decline even further after fertilisation (ICSI). This indicates that embryos largely eliminate the maternal transcripts (≥35-45 oocytes/embryos used in each group). Mean ratios are shown, with error bars representing the minimum and maximum ratio values. (C) Single nucleotide polymorphism (SNP) analysis of C57BL/6×DBA/2 embryos clearly demonstrates the presence of the paternal transcript at the 2-cell stage (blue arrowheads); maternal transcript, red arrowheads. Three different samples, each consisting of ten oocytes/embryos, were analysed for each stage. (D) The same trend was also observed for the corresponding nucleolar proteins. With the exception of B23, most of the evaluated proteins decline by the MII stage or during the 1-cell embryonic stage (zygote).

(intact *in vitro* matured oocytes). The use of ICSI allows maximum sample synchronisation. Surprisingly, real-time PCR analysis of the rRNA synthesis rate showed that nucleolus-less embryos are able to activate pre-rRNA production at the 2-cell stage at comparable levels to both controls (Fig. 2A). Therefore, the lack of RNA polymerase I activity is not the cause of the developmental arrest of nucleolus-less embryos.

It is well described in mammalian cells, as well as in yeast, that a precise balance of processed/unprocessed pre-rRNA is tightly monitored and the presence of unprocessed pre-rRNA transcripts causes various defects including cell cycle arrest and cell death (Kopp et al., 2007; Ugrinova et al., 2007; Boulon et al., 2010; Holzel et al., 2010; Chakraborty et al., 2011). We tested if aberrant pre-rRNA processing could underlie the developmental arrest.
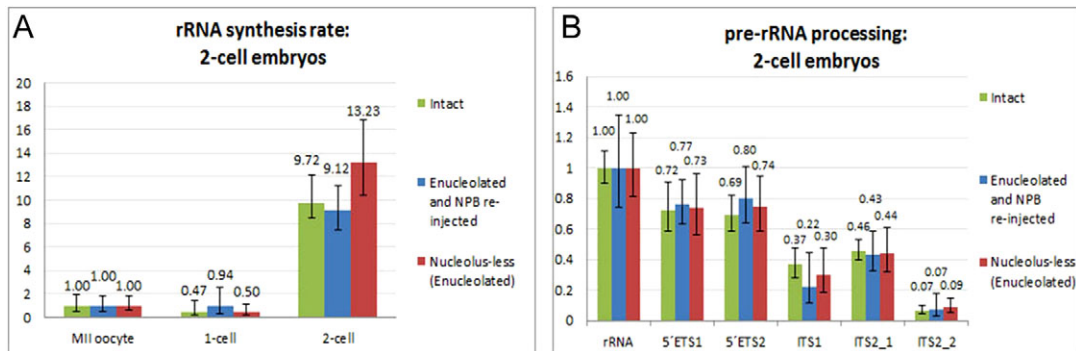
Fig. 2. Nucleolus-less embryos are able to activate rRNA synthesis. (A) Nucleolus-less embryos are able to activate rRNA synthesis at levels comparable to control embryos (intact; enucleolated with NPB re-injected). The samples were collected 6 h post-ICSI (1-cell) or 24 h post-ICSI (2-cell). At least 30 oocytes/embryos were evaluated in each group. (B) The levels of different processing products as well as unprocessed pre-rRNA were investigated. Assays targeting different regions of the pre-rRNA (5′ETS, 5′ external transcribed spacer; ITS, internal transcribed spacer) produced similar results between controls and nucleolus-less embryos at the 2-cell stage. Mean ratios are shown, with error bars representing the minimum and maximum ratio values; 40 embryos were evaluated in each group. Results of neither the rRNA synthesis rate nor processing experiments were statistically significant ($P > 0.05$, Mann-Whitney U-test).

Support for this idea comes from our observation that NPBs contain at least some proteins involved in pre-rRNA processing (B23, C23 and Fbl), but not UBF, which is essential for RNA polymerase I transcription initiation (Fig. 3). However, when the levels of different 47S pre-rRNA processing products and unprocessed transcripts were measured no difference was found between the control and experimental groups (Fig. 2B). Thus, the nucleolus-less

embryos are not only able to activate rRNA transcription but also to process the pre-rRNA transcripts produced.

Impact of enucleolation on chromosome morphology

Because this result was unexpected, we verified that we are indeed microsurgically removing the whole NPB. The protocols used to label nucleoli in somatic cells are unsuitable for labelling NPBs
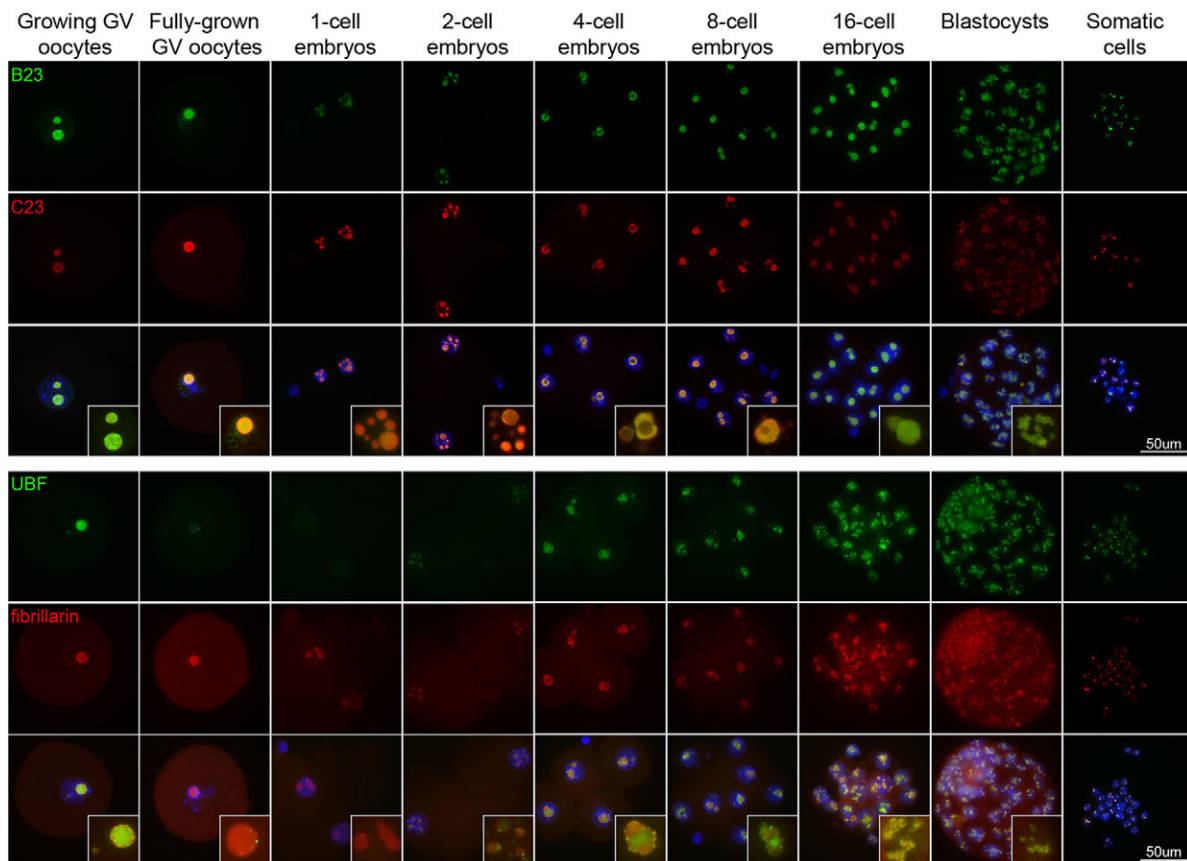

Fig. 3. The presence and localisation of nucleolar proteins in NPBs of mouse oocytes and preimplantation embryos. Antigen retrieval allows the localisation of typical nucleolar proteins involved in pre-rRNA processing (B23, C23, fibrillarin) and rRNA transcription (UBF) to NPBs in oocytes as well as in preimplantation embryos prior to genome activation. Note the decline and absence of UBF in fully grown GV oocytes and 1-cell embryos, respectively. Exposure times were kept constant, except for B23: GV oocytes, 1-cell and 2-cell embryos, 25 ms; thereafter, 10 ms. The bottom row in each case is a merge. Insets show the detail of the NPB/nucleolus.

because of their compact structure. We modified a classical antigen retrieval protocol that, combined with immunofluorescence, can be used to monitor the presence of various nucleolar proteins (Fig. 3; supplementary material Fig. S1), and we confirmed that we are indeed removing most of the maternal nucleolus, leaving on average less than 1% of the NPB material in the oocyte nucleus (Fig. 4A).

It is well known that centromeres and pericentric heterochromatin associate closely with NPBs in oocytes. In theory, these sequences might be subjected to DNA damage during enucleolation. However, at 1-2 h post-enucleolation, most of the GV oocytes did not exhibit higher levels of phosphorylated H2A.X (S139), which is a marker of DNA damage (47/56 oocytes; 84%). The percentage of phospho-H2A.X-positive oocytes (16%) matches the typical ratio of these oocytes that fails to mature to the MII stage (10-20%). The overall maturation rate is comparable between control and enucleolated oocytes. Also, no differences were found between intact and enucleolated MII oocyte chromosomes. Both groups exhibited normal chromosome morphology with prominent pericentric heterochromatin and easily detectable centromeres as well as telomeres (Fig. 4A). Typically, the chromosomal spreads contained undamaged chromosomes, although occasionally a single DNA lesion, mostly located distally, could be found [present in 16% and 17% of intact and enucleolated oocyte spreads (89 and 82 oocytes analysed), respectively]. Thus, DNA damage induced by enucleolation is unlikely to be the cause of the developmental arrest at the 2-cell stage.

Genome activation and replication during the first embryonic S phase in nucleolus-less embryos

In somatic cells, the nucleolus is involved in many cellular processes, including cell cycle progression. For this reason we used the mouse cell cycle array, which allows the simultaneous profiling of 89 selected target genes involved in cell cycle control. However, it was first necessary to verify that the nucleolus-less embryos do actually activate their genome. This was confirmed by BrUTP incorporation assay (not shown).

The expression of most of the genes investigated was not altered in nucleolus-less 2-cell embryos (including DNA damage genes such as *Atm*, *Atr*, *Brca1* and *Brca2*). The only difference was a significant downregulation of *Cdc7* and *Cdk1* [5.11-fold and 2.3-fold difference, respectively; *P*<0.05].

This prompted us to investigate whether DNA replication might be affected by NPB absence. Control and nucleolus-less zygotes were incubated with BrdU [*in vitro* fertilisation (IVF) or ICSI]. Although both groups entered S phase at approximately the same time (~6-7 h post-ICSI) and completed replication, nucleolus-less embryos (both IVF and ICSI) exhibited delayed cleavage to the 2-cell stage, as described previously (Ogushi and Saitou, 2010). The reason for this delay might be the altered chromosome morphology, especially at the pericentric chromatin region, that was detected in nucleolus-less zygotes (Fig. 4B).

Major and minor satellite sequences are affected by NPB removal

To investigate the altered chromosome morphology in more detail, we measured the content of the major and minor satellite sequences (pericentric and centric chromatin, respectively) by real-time PCR. Whereas no difference was observed between intact and enucleolated MII oocytes (Fig. 4C), 2-cell embryos originating from enucleolated oocytes exhibited decreased content of both major and minor satellite DNA (to 88% and 82%, respectively; *P*<0.05) when compared with controls (Fig. 4C). Thus, a significant

amount of satellite DNA is lost during the first embryonic cell cycle if NPBs are absent.

Because dysregulation of satellite sequence transcription leads to abnormal centromere function and, in embryos, to developmental arrest (Probst et al., 2010; Bouzinba-Segard et al., 2006), we measured the level of the satellite transcripts. Downregulation of both major and minor satellite transcripts was found in nucleolus-less embryos (Fig. 4C). This decrease was even higher than for the DNA (~2.4-fold decrease; *P*<0.05).

Parental-specific effect of NPB removal on satellite DNA and transcript levels

To dissect the roles of the parental genomes and to examine the effect of NPB removal more precisely, haploid parthenogenetic embryos were analysed. Again, a significant reduction of both major and minor satellite DNA was found in nucleolus-less parthenogenetic embryos (to 94% and 90%, respectively; *P*<0.05; Fig. 4C). Because this reduction is approximately half of that observed in biparental embryos (88% for major satellite DNA and 82% for minor satellite DNA), we conclude that the satellite DNA reduction affects both parental genomes. However, when the satellite transcript levels were measured, no marked difference between the control and the nucleolus-less group was found (Fig. 4C). Therefore, whereas the satellite DNA reduction affects both parental genomes after fertilisation, only the paternal satellite transcripts are downregulated in nucleolus-less embryos. This is in agreement with a previous report (Probst et al., 2010) that showed that it is the paternal transcript that is expressed during early embryogenesis.

Heterochromatin recombination frequency is not altered in nucleolus-less embryos

There are two possible mechanisms that could lead to the satellite DNA decrease: replication-associated loss or extensive mitotic recombination of satellite domains (Talbert and Henikoff, 2010; Jaco et al., 2008). Previously, CO-FISH (chromosome orientation fluorescence *in situ* hybridisation) was successfully applied to investigate the recombination frequencies of satellite DNA. Both control and nucleolus-less IVF embryos showed comparable frequencies of major satellite recombination events (16% and 13%, respectively; chi-squared test, *P*>0.05; Fig. 5A,B). Furthermore, no differences were found in the recombination frequency between *in vivo* produced and IVF embryos (17% and 16%, respectively; chi-squared test, *P*>0.05). However, nucleolus-less embryos exhibited distorted and irregular pericentric heterochromatin morphology, often accompanied by chromosome bridging (Fig. 5B, insets). A similar analysis was performed for the minor satellites (Fig. 5C,D). Again, comparable frequencies were found between nucleolus-less, control IVF and *in vivo* produced embryos (all 87%; chi-squared test, *P*>0.05) but again extensive chromosome bridging was observed (Fig. 5D, insets). Thus, nucleolus-less embryos fail to effectively separate chromosome bridges that form from the centric/pericentric chromatin.

Nucleolus-less embryos exhibit signs of replication stress during the first S phase and aberrant chromatin remodelling

In somatic cells and yeast, failure to separate chromosomes effectively during mitosis was observed under replication stress conditions (Sofueva et al., 2011; Chan et al., 2007, 2009). To determine whether the same applies to the nucleolus-less embryos, EdU pulse labelling followed by staining for phosphorylated histone H2A.X (S139) was used. This histone modification has been shown to be associated not only with double-strand DNA
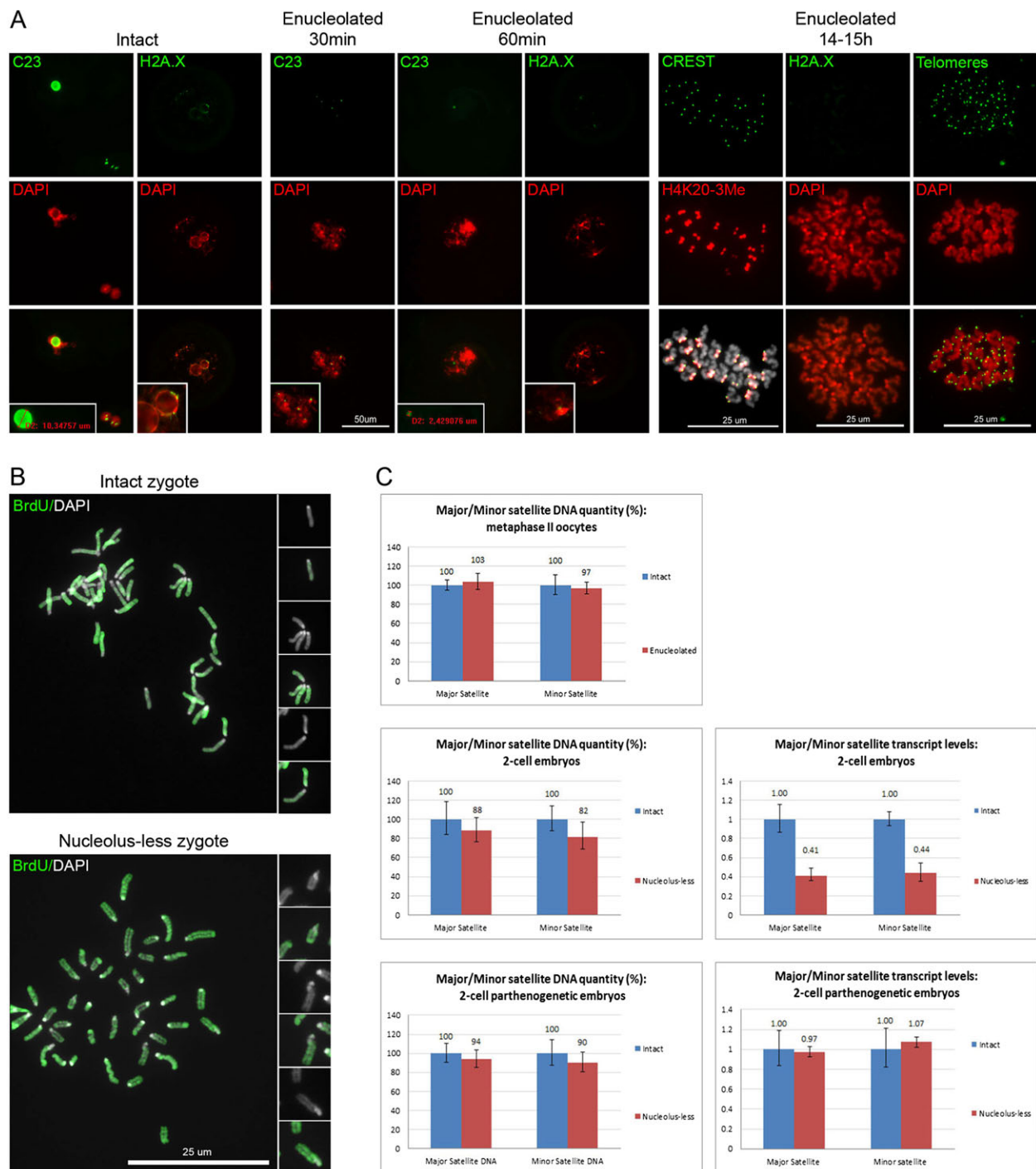
Fig. 4. The effect of NPB removal (enucleolation) on oocytes and embryos. (A) Typically, GV oocytes contain a single nucleolus, here detected by the presence of C23, and exhibit only low levels of phosphorylated H2A.X (intact). From 30 min post-enucleolation, several small C23-positive foci can be found (enucleolated 30 min). These typically fuse later on (enucleolated 60 min). The levels of phospho-H2A.X remain unchanged. Based on the diameter (insets) of the C23-positive foci the residual NPB material volume following enucleolation was estimated to be ~1% (in this case corresponding to 1.3%). Despite the close association of centromeres with nucleoli, once matured to MII, enucleolated oocytes (enucleolated 14-15 h) contain intact chromosomes (telomeres) with easily detectable pericentric chromatin (H4K20-3Me) and centromeres (CREST) and show no signs of DNA damage (H2A.X). Bottom row, merged images. In total, over 250 good spreads were analysed. (B) The first embryonic S phase occurs irrespective of nucleolus presence. However, nucleolus-less zygotes contain decompacted chromosomes with an asymmetric distribution of pericentric heterochromatin. Insets show chromosomes at higher magnification. (C) The absence of the nucleolus affects major and minor satellite DNA content and the abundance of major and minor satellite transcripts. The satellite DNA content is not influenced by the enucleolation procedure, as enucleolated and intact oocytes contain comparable levels of satellite DNA. However, this changes after the first embryonic cycle. The reduction in the satellite DNA content of parthenogenetic embryos was approximately half that of biparental embryos, whereas the transcript levels remained unchanged. Therefore, the satellite DNA loss affects both parental genomes but it is only the paternal transcript that is downregulated. The decrease of both major and minor satellite DNA/transcripts in nucleolus-less embryos (biparental/parthenogenetic) is statistically significant (*P*<0.05, Mann-Whitney U-test). Mean ratios are shown, with error bars representing the minimum and maximum ratio values; in each group 55 embryos were analysed.
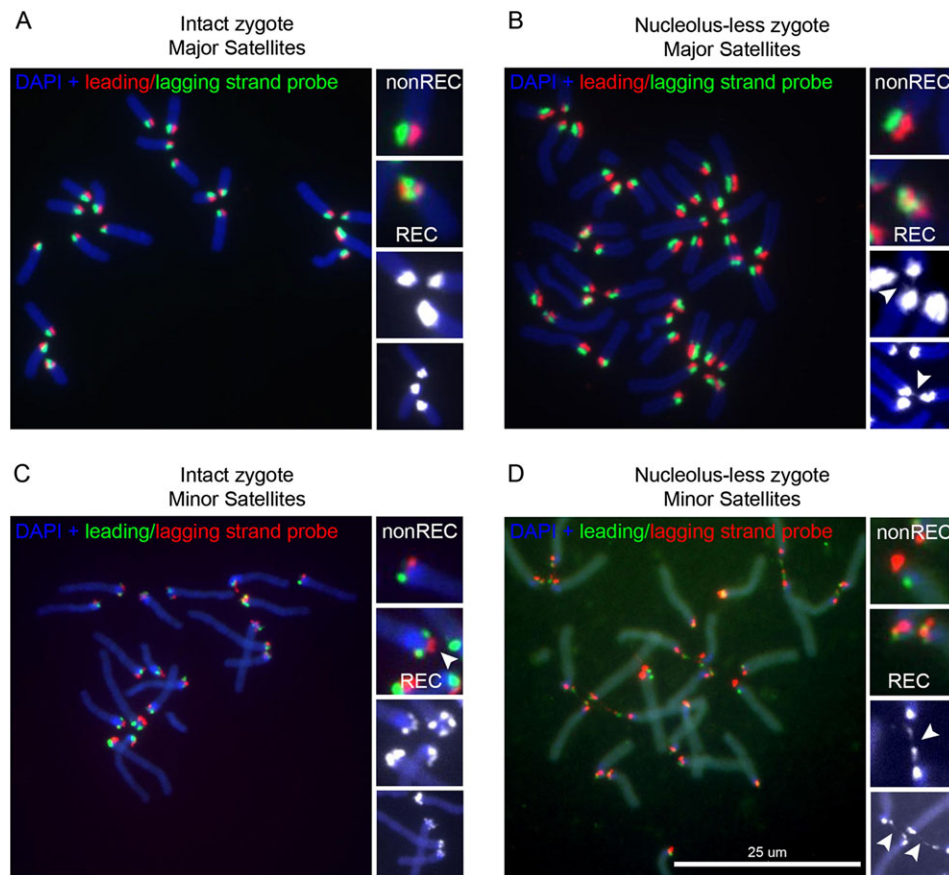
Fig. 5. NPB absence does not alter satellite recombination frequency but causes extensive chromosome bridging. (A) Major satellite sequences (pericentric chromatin) only rarely recombine in control and nucleolus-less embryos as shown by CO-FISH. Typically, separate non-interrupted signals are observed when no recombination occurs (nonREC). However, when recombination takes place the signals become overlapping or discontinuous (REC). Signals are pseudocoloured white for a better visualisation (insets). (B) A comparable recombination frequency was observed in nucleolus-less embryos. However, when closely evaluated, chromosome bridges (stretched chromatin) were found to emanate from the pericentric part of the chromosomes (insets, arrowheads). (C) In contrast to somatic cells, minor satellites (centric chromatin) were found to be highly recombinant in zygotes (insets). Again, non-recombined satellite domains are marked by separate uninterrupted signals. Chromosome bridges were found only rarely in controls (insets). (D) Also, nucleolus-less embryos show a high degree of centric chromatin recombination (discontinuous or overlapping signals) but many chromosomes remain connected together by centric chromatin bridges (insets, arrowheads). The centric chromatin bridges (highly stretched chromatin) were even more distinguishable than those of the pericentric region. Altogether, 250-700 chromosomes were evaluated in each group and experiment. Statistical analysis was performed by chi-squared test. Figure shows merged images of leading and lagging strand probe hybridization (red, green).

breaks but also with collapsing replication forks and replication stress in general (Sirbu et al., 2011; Chanoux et al., 2009; Ward and Chen, 2001). An EdU pulse was applied at different time points and zygotes were staged according to Bouniol-Baly et al. (Bouniol-Baly et al., 1997). Surprisingly, early S-phase and mid-S-phase nucleolus-less zygotes showed a weaker phospho-H2A.X signal than controls. However, as control embryos reached the end of S phase, most of the phospho-H2A.X signal was lost (Fig. 6). By contrast, a strong diffuse phospho-H2A.X signal persisted in pronuclei of nucleolus-less zygotes even after they ceased replicating. It should be noted that the nucleolus-less zygotes often exhibited replication asynchrony between pronuclei, as described previously (Bouniol-Baly et al., 1997), whereas very little replication asynchrony was observed in controls (both *in vivo* and IVF produced).

Based on the phenotype and published results, we investigated the presence and localisation of ATRX and DAXX proteins. ATRX is a maternal chromatin remodelling factor that is essential for development (Baumann et al., 2010). It contains an ATPase/helicase domain, interacts with the H3.3 histone chaperone DAXX and is necessary for recruiting it to pericentric heterochromatin in oocytes

and telomeres in somatic cells (Baumann et al., 2010; Lewis et al., 2010; Drane et al., 2010). In both enucleolated and intact GV oocytes, ATRX and DAXX were localised to DAPI-dense pericentric heterochromatin regions as described by Baumann et al. (Baumann et al., 2010). Moreover, no differences were found in chromosomes from enucleolated and control MII oocytes. After fertilisation, ATRX and DAXX localised to both pronuclei in control IVF embryos at relatively high levels. By contrast, whereas ATRX levels remained largely unchanged, markedly less DAXX could be detected in pronuclei of the nucleolus-less zygotes (Fig. 7A). When Triton X-100 permeabilisation was applied together with the fixation, the difference became even more evident (Fig. 7B). Under these conditions, in control embryos DAXX localised to the vicinity of NPBs (especially in female pronuclei), where centric/pericentric chromatin is localised, whereas no DAXX was detected in nucleolus-less zygotes. Thus, even though DAXX is transported to pronuclei in nucleolus-less zygotes it is not stably associated with DNA. This strongly suggests abnormal remodelling of the centric/pericentric chromatin in both parental pronuclei and is in agreement with the observation that satellite DNA loss affected chromosomes irrespective of their parental origin.
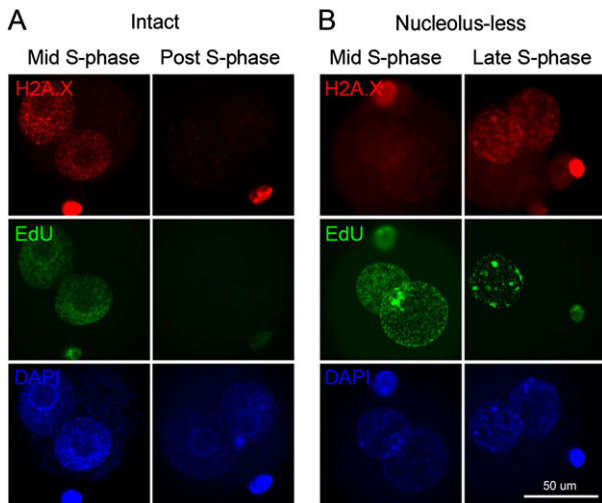
Fig. 6. Nucleolus-less embryos show a persistent phospho-H2A.X signal even after termination of DNA replication. (A) Control zygotes (intact) show a strong phospho-H2A.X signal from very early S-phase stages (here mid-S phase is shown). However, when replication is finished (post-S phase, G2) the phospho-H2A.X signal is largely lost from the pronuclei (note the absence of EdU incorporation). Overall, 126 *in vivo* and 74 *in vitro* produced embryos were evaluated at different S-phase time points. (B) Although nucleolus-less embryos initially show a lower phospho-H2A.X signal (mid-S phase) than controls, this signal persists even after the pronuclei have ceased replicating DNA (late S phase). Note that the pronuclei in nucleolus-less embryos tend to be slightly smaller than controls. Moreover, a pronounced replication asynchrony can often be observed (late S phase); here, the maternal pronucleus is finishing replication (heterochromatin) whereas the paternal pronucleus has already ceased replicating.

In summary, abnormal chromatin remodelling, replication and expression of the centric and pericentric satellite DNA accompany the developmental arrest of nucleolus-less 2-cell mouse embryos.

DISCUSSION

Altogether, our results show an unusual but essential role of the maternal nucleolus (NPB) in very early mammalian development. Contrary to our expectations, this structure does not seem to be involved in RNA polymerase I transcription activation; instead, removal of this nuclear organelle has a profound effect on the regulation of centric and pericentric DNA sequences and results in alterations in the expression profile at the time of embryonic genome activation.

Initially, we aimed to clarify the extent to which maternal nucleolar proteins and/or maternal mRNAs for nucleolar factors are used during early embryogenesis. We focused on four of the best-characterised nucleolar factors: UBF, B23, C23 and Fbl. Surprisingly, oocytes do not show a tendency to stockpile these mRNAs and proteins and their abundance is substantially reduced by the time of fertilisation or soon after. This challenges the classical view that, during their growth, oocytes make large stocks of material and that NPBs serve as the storage site of nucleolar proteins that are subsequently used by the embryo (Chouinard, 1971; and references therein). That NPBs are dispensable for rRNA synthesis is further documented by the fact that even nucleolus-less embryos are able to activate pre-rRNA production and processing at levels comparable to controls; thus, the function of NPBs during early embryogenesis is unrelated to ribosome production. To dissect the impact of NPB absence and the possible negative effect of enucleolation on rRNA production, embryos originating from intact *in vitro* matured oocytes were included in the study, but essentially no difference
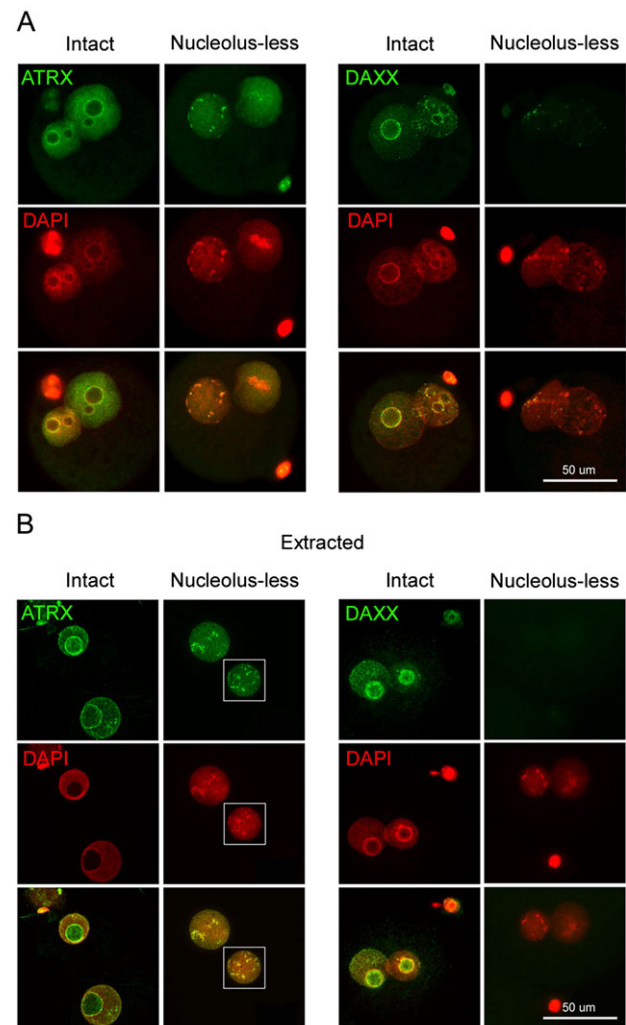

Fig. 7. NPB absence causes the loss of DAXX labelling in pronuclei. (A) Whereas ATRX was found to be present in both pronuclei irrespective of NPB presence (left), substantially less DAXX was detected in the pronuclei of nucleolus-less zygotes (right). Note the residual DAXX signal on heterochromatin. Bottom row, merged images. In total, ~70 embryos in mid-S phase were analysed in each group. (B) When detergent treatment (extracted) is applied during fixation, the DAXX labelling in nucleolus-less zygotes is completely lost (left), indicating that DAXX is not stably bound to DNA. ATRX signals remain largely unchanged even with detergent treatment (right). Boxes show the corresponding female pronucleus. Overall, at least 20 embryos in mid-S phase were analysed in each group. Bottom rows, merged images.

was detected. Therefore, enucleolation does not negatively affect these parameters. In fact, embryos lacking the nucleolus show a slightly higher pre-rRNA synthesis rate (although this difference was not statistically significant).

With respect to a possible negative impact of enucleolation, DNA damage was also examined. The majority of enucleolated oocytes showed no signs of excessive DNA damage, as only 16% exhibited a higher phospho-H2A.X signal. Because this number is comparable to the average ratio of oocytes that fail to reach the MII stage, the phospho-H2A.X-positive oocytes might simply become arrested and never reach the MII. When MII chromosomal spreads were analysed, DNA lesions were only rarely observed and were typically located distal to the centromeric part that is known to associate closely with NPBs in both oocytes and early embryos (Longo et al., 2003; Aguirre-Lavin et al., 2012). Thus, no indications of DNA damage were found

in oocytes following enucleolation. The reason for the absence of DNA damage might lie in the fact that when enucleolation is performed the oocytes are transcriptionally inactive (transcriptionally active oocytes cannot be simply enucleolated) and rDNA is probably no longer located inside NPBs (Mirre and Stahl, 1978; Vagner-Capodano et al., 1987; Zatsepina et al., 2000). In agreement with this, Kyogoku et al. (Kyogoku et al., 2011) showed that, if actinomycin D is used to block RNA polymerase I activity in transcriptionally active oocytes, such oocytes can also be enucleolated.

Overall, very few differences between control and nucleolus-less embryos were found. The only clear variation was the altered chromosome morphology that was apparent when zygotes were analysed. Specifically, we noted changes in chromosome condensation and asymmetric pericentric heterochromatin distribution. We found reduced satellite DNA in both IVF and ICSI biparental and parthenogenetic nucleolus-less embryos. However, the reduction in satellite transcripts was observed only in embryos containing the paternal genome and not in parthenotes. Because parthenogenetic embryos also fail to develop beyond the 2-cell stage, the reduction in satellite transcripts does not appear to be the only cause of developmental arrest. Altered satellite transcript levels have, however, been reported to be important for restructuring male centromeres (Probst et al., 2010). The role of the maternal nucleolus in this process has not been described previously.

We then focused on the potential mechanism of the satellite DNA reduction. Generally, there are two possible explanations: the first is extensive mitotic recombination of the satellites; the second, aberrant replication and/or remodelling (Chan et al., 2009; Lukas et al., 2011; Talbert and Henikoff, 2010).

The overall recombination frequencies were similar between control and experimental embryos. Therefore, extensive mitotic recombination is unlikely to be the reason for the developmental arrest. Interestingly, the recombination frequency of minor satellites seems to be much higher in zygotes (on average ~87% of these sequences were found to be recombinant) compared with somatic cells, where the frequency ranges from 15% to 20% (Jaco et al., 2008). This is unlikely to be caused by any differences in the methodology and/or probes used because we followed the published protocol in detail and our preliminary experiments in parthenogenetic embryos showed a much lower recombination frequency. Whether this high recombination frequency is the result of combining two different parental genomes after fertilisation remains to be elucidated. Although the major satellite recombination rate in somatic cells is not known precisely, in our system it was ~16-17% and was roughly comparable to the minor satellite recombination frequency in somatic cells. Again, no difference in the frequency was observed between experimental and control groups.

The second potential mechanism of satellite DNA loss might include abnormal first embryonic S-phase progression. Indeed, an altered dynamics of phospho-H2A.X deposition during this phase was observed in nucleolus-less embryos. Although there is some discrepancy in the literature with respect to the presence of phospho-H2A.X in mouse zygotes, our results in control embryos are in agreement with several published articles in which this histone modification was closely monitored (e.g. Wossidlo et al., 2010; Ziegler-Birling et al., 2009).

Bouniol-Baly et al. (Bouniol-Baly et al., 1997) described that the paternal pronucleus initiates and finishes DNA replication earlier than the maternal pronucleus. Interestingly, when we followed the patterns of EdU incorporation at different time points the described replication asynchrony between pronuclei was observed in nucleolus-less zygotes only. By contrast, such a marked replication asynchrony

was never observed in control zygotes (both *in vivo* and IVF produced) under our conditions. Indeed, several articles questioning the replication asynchrony have been published (Yamauchi et al., 2009; and references therein). For example, Yamauchi et al. (Yamauchi et al., 2009) reported that, even though mouse zygotes can tolerate asynchronous DNA replication in their pronuclei, this does not normally occur after IVF or ICSI.

An interesting phenomenon has been described in yeast *cdc14* mutants. Cdc14 is a cell cycle regulatory protein that localises to nucleoli throughout most of the cell cycle. These yeast mutants exhibit heterochromatin under-replication but this does not trigger cell cycle checkpoints and does not alter replication-associated gene expression immediately; rather, this defect is manifested during the next cell cycle (Dulev et al., 2009). Essentially the same situation was observed in our system, including the changes in replication-associated transcripts at the 2-cell stage. However, the alteration in gene expression at this stage might be primarily related to the fact that the major genome activation occurs at this time, and the lag in gene expression change might be simply explained by the presence of maternal transcripts and/or proteins that are involved in sustaining the first embryonic cell cycle. Currently, we cannot exclude this possibility.

In addition to the replication-associated changes, the alteration in gene expression and the satellite DNA loss in nucleolus-less embryos, we show that the absence of the NPB causes extensive chromosome bridging during the first embryonic mitosis. The reason why we initially did not observe these fine satellite bridges in our primary replication/karyotype analysis might be related to the use of HCl in the BrdU assay. It is well known that HCl causes DNA hydrolysis and thus might have caused the loss of these DNA bridges. However, the use of CO-FISH with peptide nucleic acid (PNA) probes that require minimal or no denaturation of target DNA allowed their detection. Interestingly, both minor and major (centric and pericentric) satellite sequences were involved in this bridging. This contrasts with results obtained in somatic cells, as only centric chromatin was indicated to be involved in ultrafine bridge formation (Baumann et al., 2007; Chan et al., 2007). Recent results in somatic cells show that the formation of chromosome bridges is relatively common, even under optimal conditions, but is enhanced significantly with replication stress. Indeed, when we analysed closely chromosomal preparations from zygotes these bridges were present even in control embryos. Typically, 0-3 bridged pairs were found per 40 chromosomes (on average ~8% of all chromosomes evaluated were involved in bridging). By contrast, in nucleolus-less embryos the vast majority of chromosomes were affected (sometimes as many as 38 out of 40 chromosomes were bridged) and the overall frequency was 78%. Chan et al. (Chan et al., 2007) proposed two possible models to explain DNA bridge formation: the sequences are either fully replicated but fail to separate (catenate) or they are only partially replicated and thus the DNA remains hemicatenated. If we apply the first model to our system, then chromosome bridging would have to be followed by massive DNA degradation because nearly 20% of the minor satellites is lost between the 1- and 2-cell embryonic stages (plus the concomitant major satellite loss). However, recent results in somatic cells do not support the degradation model, as the DNA lesions were shown to be protected by a protein sheltering mechanism and are effectively repaired in the subsequent G1 phase (Lukas et al., 2011).

Concomitantly, we show that the H3.3 histone chaperone DAXX fails to stably bind to DNA in nucleolus-less zygotes. This strongly implies abnormal or absent remodelling of the satellite sequences. In contrast to somatic cells, where H3.3 is incorporated into DNA in a replication-independent manner, recent results in embryos show that H3.3 incorporation occurs even during S phase (Akiyama et al.,

2011; Santenard et al., 2010). This is understandable given the necessity of extensive remodelling of both parental genomes after fertilisation. Unfortunately, no anti-H3.3-specific antibodies are currently available and the direct test cannot be performed readily. Our results are in agreement with those of Santenard et al. (Santenard et al., 2010), who injected mRNA for different histone H3 variants into embryos. They showed that H3.3 is specifically necessary for the remodelling of centromeres and the introduction of a mutant version causes developmental arrest.

DAXX forms a complex with ATRX and this is necessary for its correct targeting (Drane et al., 2010; Lewis et al., 2010; Baumann et al., 2010). In nucleolus-less embryos, however, ATRX localisation remains unaffected. Therefore, it is highly probable that there are additional – presumably nucleolar – proteins involved and engaged in another level of ATRX/DAXX regulation. This, however, remains to be investigated.

Taken together, our data show an unusual and previously unappreciated role of the maternal nucleolus in early mammalian embryogenesis.

MATERIALS AND METHODS
Oocyte and embryo collection
Mice (C57BL/6 and B6D2F1; Charles River Laboratories) were kept under standard housing conditions with 12 h light/dark cycle (light on at 8:00 a.m.). Females were injected intraperitoneally with 7.5 I.U. PMSG (Calbiochem). After 44 h, mice were sacrificed by cervical dislocation and GV stage oocytes were released from follicles into HTF-HEPES medium (Zenith Biotech). The oocytes were then cultured in MEM medium supplemented with gentamicin (50 µg/ml), sodium pyruvate (0.22 mM), dibutyryl cyclic adenosine monophosphate (dbcAMP; 150 µg/ml) and bovine serum albumin (BSA; 4 mg/ml) at 37°C in an atmosphere of 5% CO_2 and used for further manipulations. Alternatively, after a brief culture, oocytes were either washed in phosphate buffered saline (PBS)/0.1% polyvinyl alcohol (PVA), collected in Laemmli sample buffer and used for western blotting or fixed and used for immunofluorescence.

MII oocytes were obtained from stimulated females [7.5 I.U. PMSG, followed by 7.5 I.U. hCG (Intervet) 48 h later]. Ovulated oocytes were collected from ampulae of sacrificed mice.

In vivo produced embryos were obtained from stimulated females as above, except that after hCG injection females were caged with males. Next morning, females were sacrificed and 1-cell stage embryos were released from ampulae into HTF-HEPES medium and further cultured in KSOM medium (Zenith Biotech).

Enucleolation and intracytoplasmic sperm injection (ICSI)
Enucleolation of GV stage oocytes and nucleolus re-injection were performed essentially as described (Fulka et al., 2003). Enucleolated and control (nucleolus re-injected) oocytes were allowed to recover in MEM supplemented with dbcAMP (to prevent GV breakdown) for 30 min or 1 h and used for immunofluorescence. Alternatively, manipulated oocytes were washed free of dbcAMP and cultured in MEM medium to MII. The MII oocytes were used for ICSI as described (Yoshida and Perry, 2007) and then cultured in KSOM medium. ICSI was used especially in experiments in which maximum embryo synchronisation was required (e.g. rRNA production and processing, gene expression profiling).

In vitro fertilisation (IVF)
IVF of *in vitro* matured MII oocytes (manipulated and control) was carried out as described (Takeo and Nakagata, 2011). Fresh sperm from cauda epididymides of DBA/2 male mice (minimum 8 weeks old) were used.

Parthenogenetic activation
Parthenogenetic activation of MII oocytes was performed as described (Kishigami and Wakayama, 2007) except that the activation was carried out in KSOM medium and cytochalasin B was omitted.

BrdU incorporation
Embryos were incubated in medium supplemented with 5-bromo-2′-deoxyuridine (BrdU; 50 µm). Embryos were fixed in 4% paraformaldehyde (PFA) for 10 min and processed for immunofluorescence. Alternatively, demecolcine was added (0.1 µg/ml; Sigma-Aldrich) in order to arrest embryos at the first embryonic mitosis. Chromosomal spreads were prepared as described (Kamiguchi and Mikano, 1986). A short incubation in 4 M HCl (15 min) followed by immunofluorescence was used to detect BrdU. YOYO-1 (10 nM; Life Technologies) labelling for 10 min was used to counterstain the chromosomes.

Conventional immunofluorescence
Zona pellucida-free oocytes/embryos were fixed in 4% PFA in PBS for 15 min and permeabilised by 0.2% Triton X-100 in PBS. After blocking in 1% BSA in PBS, the samples were incubated with selected primary antibodies overnight at 4°C, washed, incubated with secondary antibodies, mounted in ProLong Gold supplemented with DAPI (Life Technologies) and evaluated under an Olympus IX71 microscope. The images were captured by ImagePro software (Media Cybernetics) and processed by Adobe Photoshop. Antibodies used: anti-BrdU (Roche, 11170376001; 1:100; also used for BrUTP detection), anti-ATRX and anti-DAXX (Santa Cruz Biotechnology, sc-15408 and sc-7152; both 1:500), anti-γH2A.X (Millipore, 05-636-I; 1:2000). All secondary antibodies were purchased from Jackson ImmunoResearch; a 1 h incubation at 37°C or room temperature was used.

Chromosome spreading and antigen retrieval (AR)
Oocytes and embryos were gently spread on SuperFrost slides as described (Hodges and Hunt, 2002). The slides were either used directly for immunofluorescence or AR was first performed. For AR, the slides were boiled in 10 mM sodium citrate containing 0.05% Tween 20 (pH 6.0) for 15 min, briefly washed in PBS and blocked/permeabilised as above. Primary antibody incubation was performed for 1 h at 37°C. The samples were examined under an Olympus BX61 microscope. Antibodies used: anti-ATRX, anti-DAXX and anti-γH2A.X (see above), anti-C23 (Abcam, ab70493; 1:400), anti-B23 (Sigma-Aldrich, B0556; 1:200), anti-Fibrillarin (Cell Signaling, mAB#2639; 1:400), anti-UBF (Abnova, H00007343-M01; 1:200), anti-H4/K20-3Me (Abcam, ab9053; 1:2000), CREST antiserum (Fitzgerald Industries International, 90C-CS1058; 1:1000), anti-SC35 (Sigma-Aldrich, S4045; 1:200), anti-nuclear pore complex (NPC; Covance, MAb414; 1:100). Secondary antibodies were as above.

BrUTP injection
For the assessment of general transcription, embryos were injected with 5-bromouridine-5′-triphosphate (BrUTP) as described (Bouniol-Baly et al., 1997). After 1 h incubation, the embryos were fixed in 4% PFA and nascent transcripts were detected by immunofluorescence.

Telomere peptide nucleic acid (PNA) fluorescence *in situ* hybridisation (FISH)
Chromosome spreads were prepared as described above. FISH was performed according to the PNA probe manufacturer (Panagene). TelC-Cy3 probe was used.

Chromosome orientation FISH (CO-FISH)
CO-FISH was performed as described (Jaco et al., 2008; Falconer et al., 2010). In brief, this method involves the incorporation of BrdU into DNA followed by UV exposure and enzymatic degradation of the newly synthesized strand. When such chromosomes are hybridised to oppositely oriented probes (coupled to different dyes) separate uninterrupted non-overlapping signals are obtained if no recombination has occurred.

EdU labelling
5-ethynyl-2′-deoxyuridine (EdU) labelling was performed as recommended by the manufacturer (Life Technologies) except that 100 µM EdU was added to the KSOM medium for 1 h. Subsequently, conventional immunofluorescence was performed as described above.

Western blotting

Samples of 100 mouse oocytes or embryos were separated by 10% SDS-PAGE. A control sample of 1 µg total 3T3A31 cell lysate was included. Proteins were transferred onto a PVDF membrane (GE Healthcare), which was blocked in 5% nonfat dried milk (Bio-Rad) in Tris-buffered saline supplemented with 0.1% Tween 20 (TBST). Antibodies used were: anti-UBF (1:5000), anti-B23 (1:2000), anti-fibrillarin (1:1000), anti-C23 (1:2000) and anti-α-tubulin (Sigma-Aldrich, T6074, 1:2000). HRP-conjugated secondary antibody was obtained from Bio-Rad. Proteins were visualised using the ECL Advance Western Blotting Detection Kit (GE Healthcare) as recommended by the manufacturer.

RT-PCR and real-time PCR

Samples of five oocytes/embryos were processed using the FastLane Cell RT-PCR Kit (Qiagen) as recommended by the manufacturer, snap-frozen in liquid nitrogen and stored −80°C until use. A genomic DNA elimination step was performed followed by reverse transcription (RT) with random hexamers and SuperScript III reverse transcriptase (Life Technologies) according to the manufacturer's instructions. Synthetic EGFP mRNA was added to the sample prior to RT. No-RT controls were also evaluated. The reaction was diluted and 2 µl used for PCR with Power SYBR Green Master Mix (Life Technologies). Total PCR volume was 20 µl. Serial dilution of the template was used to determine the PCR efficiencies for data evaluation according to Pfaffl (Pfaffl, 2001). Primers are listed in supplementary material Table S1. PCR was performed using the 7900HT Fast Real-Time PCR System (Life Technologies) with cycling conditions: 95°C 10 min, followed by 40 cycles of 95°C for 15 s and 59°C for 1 min. Expression values are given as relative ratios±minimum and maximum relative ratios. All PCR products were cloned using the TOPO-TA Cloning Kit For Sequencing (Life Technologies) and sequenced.

SNP analysis

cDNA was amplified with PerfectTag polymerase (5 PRIME). The PCR product was digested by *Van*91I (C23) or *Hha*I (UBF) (Fermentas) and analysed on either 4% TBE agarose (C23) or on standard PAGE (UBF, Ubtf) gels. In both cases, SybrSafe (Life Technologies) was used to visualise the fragments.

Major/minor satellite real-time PCR

To investigate the content of major and minor satellite sequences, embryos were allowed to pass through the first embryonic S phase (zygotes) and were collected at the very early 2-cell stage (after the first replication but prior to the second round, ~22 h after ICSI or IVF). Genomic DNA was isolated as described (Zuccotti and Monk, 1995) and the lysate was amplified by real-time PCR as described (Zhu et al., 2011). Alternatively, cDNA from 2-cell embryos was used as a template. To monitor replication *36B4* (*Rplp0*) was used, a well-characterised single-copy gene that is often used in quantitative telomeric assays (Callicott and Womack, 2006). The major and minor satellite primer sets were validated for both DNA and RNA. The results were subjected to statistical analysis (Mann-Whitney test). For real-time PCR analysis at least nine different measurements were evaluated in each group.

Gene expression profiling

Samples of five embryos were collected as for real-time PCR analysis. Reverse transcription was performed with the RT[2] PreAMP cDNA Synthesis Kit and RT[2] PreAMP Pathway Primer Mix (SABiosciences, now Qiagen) as described by the manufacturer. The Mouse Cell Cycle Array (PAMM-020ZC) was used for gene expression analysis (SABiosciences). Results were evaluated with the help of the SABiosciences Excel application designed for this array.

Author contributions
H.F. conceived the study, designed and performed experiments and wrote the manuscript. A.L. performed the oocyte manipulations and immunofluorescence.

References

Aguirre-Lavin, T., Adenot, P., Bonnet-Garnier, A., Lehmann, G., Fleurot, R., Boulesteix, C., Debey, P. and Beaujean, N. (2012). 3D-FISH analysis of embryonic nuclei in mouse highlights several abrupt changes of nuclear organization during preimplantation development. *BMC Dev. Biol.* **12**, 30.

Akiyama, T., Suzuki, O., Matsuda, J. and Aoki, F. (2011). Dynamic replacement of histone H3 variants reprograms epigenetic marks in early mouse embryos. *PLoS Genet.* **7**, e1002279.

Baumann, C., Körner, R., Hofmann, K. and Nigg, E. A. (2007). PICH, a centromere-associated SNF2 family ATPase, is regulated by Plk1 and required for the spindle checkpoint. *Cell* **128**, 101-114.

Baumann, C., Viveiros, M. M. and De La Fuente, R. (2010). Loss of maternal ATRX results in centromere instability and aneuploidy in the mammalian oocyte and pre-implantation embryo. *PLoS Genet.* **6**, e1001137.

Biggiogera, M., Martin, T. E., Gordon, J., Amalric, F. and Fakan, S. (1994). Physiologically inactive nucleoli contain nucleoplasmic ribonucleoproteins: immunoelectron microscopy of mouse spermatids and early embryos. *Exp. Cell Res.* **213**, 55-63.

Boulon, S., Westman, B. J., Hutten, S., Boisvert, F.-M. and Lamond, A. I. (2010). The nucleolus under stress. *Mol. Cell* **40**, 216-227.

Bouniol-Baly, C., Nguyen, E., Besombes, D. and Debey, P. (1997). Dynamic organization of DNA replication in one-cell mouse embryos: relationship to transcriptional activation. *Exp. Cell Res.* **236**, 201-211.

Bouzinba-Segard, H., Guais, A. and Francastel, C. (2006). Accumulation of small murine minor satellite transcripts leads to impaired centromeric architecture and function. *Proc. Natl. Acad. Sci. U.S.A.* **103**, 8709-8714.

Callicott, R. and Womack, J. E. (2006). Real-time PCR assay for measurement of mouse telomeres. *Comp. Med.* **56**, 17-22.

Chakraborty, A., Uechi, T. and Kenmochi, N. (2011). Guarding the 'translation apparatus': defective ribosome biogenesis and the p53 signaling pathway. *Wiley Interdiscip. Rev. RNA* **2**, 507-522.

Chan, K.-L., North, P. S. and Hickson, I. D. (2007). BLM is required for faithful chromosome segregation and its localization defines a class of ultrafine anaphase bridges. *EMBO J.* **26**, 3397-3409.

Chan, K. L., Palmai-Pallag, T., Ying, S. and Hickson, I. D. (2009). Replication stress induces sister-chromatid bridging at fragile site loci in mitosis. *Nat. Cell Biol.* **11**, 753-760.

Chanoux, R. A., Yin, B., Urtishak, K. A., Asare, A., Bassing, C. H. and Brown, E. J. (2009). ATR and H2AX cooperate in maintaining genome stability under replication stress. *J. Biol. Chem.* **284**, 5994-6003.

Chouinard, L. A. (1971). A light- and electron-microscope study of the nucleolus during growth of the oocyte in the prepubertal mouse. *J. Cell Sci.* **9**, 637-663.

Drane, P., Ouararhni, K., Depaux, A., Shuaib, M. and Hamiche, A. (2010). The death-associated protein DAXX is a novel histone chaperone involved in the replication-independent deposition of H3.3. *Genes Dev.* **24**, 1253-1265.

Dulev, S., de Renty, C., Mehta, R., Minkov, I., Schwob, E. and Strunnikov, A. (2009). Essential global role of CDC14 in DNA synthesis revealed by chromosome underreplication unrecognized by checkpoints in cdc14 mutants. *Proc. Natl. Acad. Sci. U.S.A.* **106**, 14466-14471.

Falconer, E., Chavez, E. A., Henderson, A., Poon, S. S. S., McKinney, S., Brown, L., Huntsman, D. G. and Lansdorp, P. M. (2010). Identification of sister chromatids by DNA template strand sequences. *Nature* **463**, 93-97.

Fulka, J., Jr, Moor, R. M., Loi, P. and Fulka, J. (2003). Enucleolation of porcine oocytes. *Theriogenology* **59**, 1879-1885.

Hodges, C. A. and Hunt, P. A. (2002). Simultaneous analysis of chromosomes and chromosome-associated proteins in mammalian oocytes and embryos. *Chromosoma* **111**, 165-169.

Holzel, M., Orban, M., Hochstatter, J., Rohrmoser, M., Harasim, T., Malamoussi, A., Kremmer, E., Langst, G. and Eick, D. (2010). Defects in 18 S or 28 S rRNA processing activate the p53 pathway. *J. Biol. Chem.* **285**, 6364-6370.

Jaco, I., Canela, A., Vera, E. and Blasco, M. A. (2008). Centromere mitotic recombination in mammalian cells. *J. Cell Biol.* **181**, 885-892.

Kamiguchi, Y. and Mikano, K. (1986). An improved, efficient method for analyzing human sperm chromosomes using zona-free hamster ova. *Am. J. Hum. Genet.* **38**, 724-740.

DEVELOPMENT

Kishigami, S. and Wakayama, T. (2007). Efficient strontium-induced activation of mouse oocytes in standard culture media by chelating calcium. *J. Reprod. Dev.* **53**, 1207-1215.

Kopp, K., Gasiorowski, J. Z., Chen, D., Gilmore, R., Norton, J. T., Wang, C., Leary, D. J., Chan, E. K. L., Dean, D. A. and Huang, S. (2007). Pol I transcription and pre-rRNA processing are coordinated in a transcription-dependent manner in mammalian cells. *Mol. Biol. Cell* **18**, 394-403.

Kyogoku, H., Ogushi, S., Miyano, T. and Fulka, J., Jr (2011). Nucleoli from growing oocytes inhibit the maturation of enucleolated, full-grown oocytes in the pig. *Mol. Reprod. Dev.* **78**, 426-435.

Lewis, P. W., Elsaesser, S. J., Noh, K.-M., Stadler, S. C. and Allis, C. D. (2010). Daxx is an H3.3-specific histone chaperone and cooperates with ATRX in replication-independent chromatin assembly at telomeres. *Proc. Natl. Acad. Sci. U.S.A.* **107**, 14075-14080.

Longo, F., Garagna, S., Merico, V., Orlandini, G., Gatti, R., Scandroglio, R., Redi, C. A. and Zuccotti, M. (2003). Nuclear localization of NORs and centromeres in mouse oocytes during folliculogenesis. *Mol. Reprod. Dev.* **66**, 279-290.

Lukas, C., Savic, V., Bekker-Jensen, S., Doil, C., Neumann, B., Pedersen, R. S., Gröfte, M., Chan, K. L., Hickson, I. D., Bartek, J. et al. (2011). 53BP1 nuclear bodies form around DNA lesions generated by mitotic transmission of chromosomes under replication stress. *Nat. Cell Biol.* **13**, 243-253.

Mirre, C. and Stahl, A. (1978). Ultrastructure and activity of the nucleolar organizer in the mouse oocyte during meiotic prophase. *J. Cell Sci.* **31**, 79-100.

Ogushi, S. and Saitou, M. (2010). The nucleolus in the mouse oocyte is required for the early step of both female and male pronucleus organization. *J. Reprod. Dev.* **56**, 495-501.

Ogushi, S., Palmieri, C., Fulka, H., Saitou, M., Miyano, T. and Fulka, J., Jr (2008). The maternal nucleolus is essential for early embryonic development in mammals. *Science* **319**, 613-616.

Pfaffl, M. W. (2001). A new mathematical model for relative quantification in real-time RT-PCR. *Nucleic Acids Res.* **29**, e45.

Pochukalina, G. N. and Parfenov, V. N. (2008). Nucleolus transformation in mouse antral follicles: distribution of coilin and components of RNA-polymerase I complex. *Cell Tissue Biol.* **2**, 522-530.

Probst, A. V., Okamoto, I., Casanova, M., El Marjou, F., Le Baccon, P. and Almouzni, G. (2010). A strand-specific burst in transcription of pericentric satellites is required for chromocenter formation and early mouse development. *Dev. Cell* **19**, 625-638.

Santenard, A., Ziegler-Birling, C., Koch, M., Tora, L., Bannister, A. J. and Torres-Padilla, M.-E. (2010). Heterochromatin formation in the mouse embryo requires critical residues of the histone variant H3.3. *Nat. Cell Biol.* **12**, 853-862.

Sirbu, B. M., Couch, F. B., Feigerle, J. T., Bhaskara, S., Hiebert, S. W. and Cortez, D. (2011). Analysis of protein dynamics at active, stalled, and collapsed replication forks. *Genes Dev.* **25**, 1320-1327.

Sofueva, S., Osman, F., Lorenz, A., Steinacher, R., Castagnetti, S., Ledesma, J. and Whitby, M. C. (2011). Ultrafine anaphase bridges, broken DNA and illegitimate recombination induced by a replication fork barrier. *Nucleic Acids Res.* **39**, 6568-6584.

Takeo, T. and Nakagata, N. (2011). Reduced glutathione enhances fertility of frozen/thawed C57BL/6 mouse sperm after exposure to methyl-beta-cyclodextrin. *Biol. Reprod.* **85**, 1066-1072.

Talbert, P. B. and Henikoff, S. (2010). Centromeres convert but don't cross. *PLoS Biol.* **8**, e1000326.

Ugrinova, I., Monier, K., Ivaldi, C., Thiry, M., Storck, S., Mongelard, F. and Bouvet, P. (2007). Inactivation of nucleolin leads to nucleolar disruption, cell cycle arrest and defects in centrosome duplication. *BMC Mol. Biol.* **8**, 66.

Vagner-Capodano, A. M., Hartung, M. and Stahl, A. (1987). Nucleolus, nucleolar chromosomes, and nucleolus-associated chromatin from early diplotene to dictyotene in the human oocyte. *Hum. Genet.* **75**, 140-146.

Ward, I. M. and Chen, J. (2001). Histone H2AX is phosphorylated in an ATR-dependent manner in response to replicational stress. *J. Biol. Chem.* **276**, 47759-47762.

Wossidlo, M., Arand, J., Sebastiano, V., Lepikhov, K., Boiani, M., Reinhardt, R., Schöler, H. and Walter, J. (2010). Dynamic link of DNA demethylation, DNA strand breaks and repair in mouse zygotes. *EMBO J.* **29**, 1877-1888.

Yamauchi, Y., Ward, M. A. and Ward, W. S. (2009). Asynchronous DNA replication and origin licensing in the mouse one-cell embryo. *J. Cell. Biochem.* **107**, 214-223.

Yoshida, N. and Perry, A. C. F. (2007). Piezo-actuated mouse intracytoplasmic sperm injection (ICSI). *Nat. Protoc.* **2**, 296-304.

Zatsepina, O. V., Bouniol-Baly, C., Amirand, C. and Debey, P. (2000). Functional and molecular reorganization of the nucleolar apparatus in maturing mouse oocytes. *Dev. Biol.* **223**, 354-370.

Zhu, Q., Pao, G. M., Huynh, A. M., Suh, H., Tonnu, N., Nederlof, P. M., Gage, F. H. and Verma, I. M. (2011). BRCA1 tumour suppression occurs via heterochromatin-mediated silencing. *Nature* **477**, 179-184.

Ziegler-Birling, C., Helmrich, A., Tora, L. and Torres-Padilla, M.-E. (2009). Distribution of p53 binding protein 1 (53BP1) and phosphorylated H2A.X during mouse preimplantation development in the absence of DNA damage. *Int. J. Dev. Biol.* **53**, 1003-1011.

Zuccotti, M. and Monk, M. (1995). Methylation of the mouse Xist gene in sperm and eggs correlates with imprinted Xist expression and paternal X-inactivation. *Nat. Genet.* **9**, 316-320.
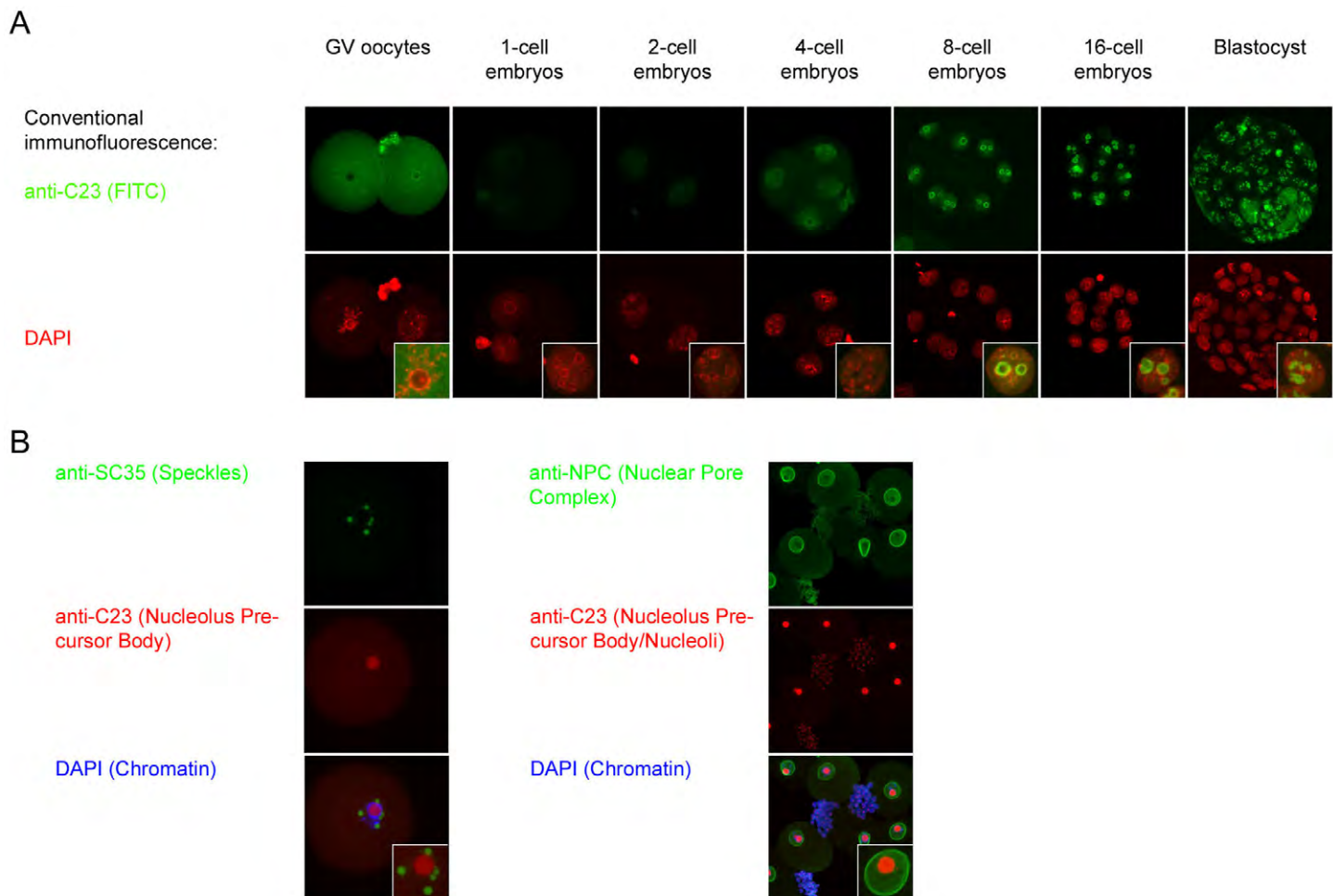
DEVELOPMENT

Figure S1. The comparison of NPB labelling strategies by conventional immunofluorescence protocols and antigen retrieval/ immunofluorescence protocol. (A) The use of conventional protocols does not allow staining of the inside of NPBs as antibodies are unable to penetrate the dense structure. Typically, positive staining of the nucleolus is obtained from the time of embryonic genome activation onwards (2- to 4-cell embryos). (B) The use of antigen retrieval combined with immunofluorescence results in NPB labelling even in GV stage oocytes. Moreover, this protocol does not cause unspecific reactivity of the NPB to other antibodies (e.g. anti-SC35 or anti-NPC).

Table S1. Primers used for real-time PCR and SNP analysis

Primer	Sequence	Concentration	Location
rRNA_F	GGTGTCCAAGTGTTCATGC	600 nM	5´external transcribed spacer
rRNA_R	CAAGCGAGATAGGAATGTCTTAC	900 nM	5´external transcribed spacer
5ETS_F1	TGTTTCACTTTGGTCGTGTCTC	600 nM	5´external transcribed spacer
5ETS_R1	TCGACGCTTACAAGAAACAGC	600 nM	5´external transcribed spacer
5ETS_F2	GTCTTCTGGTTTCCCTGTGTG	900 nM	5´external transcribed spacer
5ETS_R2	GCTAGAGAAGGAAACTTTCTCACTG	600 nM	5´external transcribed spacer
ITS1_F	TCTCGTTTCGTTCCTGCTGG	900 nM	internal transcribed spacer 1/5.8S rRNA
ITS1_R	GATCCACCGCTAAGAGTCGTATC	900 nM	internal transcribed spacer 1/5.8S rRNA
ITS2_F1	GAGAACGGAGAGAGGTGGTATC	300 nM	internal transcribed spacer 2
ITS2_R1	AGAAGCGGAGACGAAGAAGAG	300 nM	internal transcribed spacer 2
ITS2_F2	CGTGTGAGTAAGATCCTCCAC	900 nM	internal transcribed spacer 2/28S rRNA
ITS2_R2	GTTACTGAGGGAATCCTGGTTAG	600 nM	internal transcribed spacer 2/28S rRNA
EGFP_F	CACCATCTTCTTCAAGGACG	900 nM	
EGFP_R	GTGGCTGTTGTAGTTGTACTC	300 nM	
C23_SNP_F	CACACCAGCTAAGAAAAACATTACAC	300 nM	Exon 2/3
C23_SNP_R	ACTCATCCTCTTCCTCATCATCTTC	300 nM	Exon 2/3
UBF_SNP_F	GAGAAGAAGAAGGCTAAATACAAGG	300 nM	Exon 10/11
UBF_SNP_R	TCACCCGGTCATTCTTGAAG	300 nM	Exon 10/11